$\pi^- p \to \gamma\gamma n$ in a chiral Lagrangian model

J. B. Cammarata
Department of Physics, Virginia Polytechnic Institute, Blacksburg, Virginia 24061
(Received 19 March 1979)

Using a chiral Lagrangian we have evaluated the tree diagrams for $\pi^- p \to \gamma\gamma n$. With this model we have studied the feasibility of using an experiment which detects only the final state gammas to resolve two matters of theoretical interest: the off-mass-shell behavior of the πN amplitude and the sign of the $\pi^0 \to \gamma\gamma$ amplitude. Our results suggest that this reaction is not a practicable way to distinguish between different models of the off-mass-shell amplitude, but that a reasonably accurate experiment could determine the sign of the π^0 decay amplitude.

[NUCLEAR REACTIONS $p(\pi^-, \gamma\gamma)n$; inflight capture; $T_\pi^{\text{lab}} \leq 100$ MeV; chiral Lagrangian model; calculated $\sigma(\theta)$; two photon detection. Studied effects of off-mass-shell πN amplitude and sign of $\pi^0 \to \gamma\gamma$ amplitude.]

I. INTRODUCTION

Recent experiments have detected, for the first time, the simultaneous emission of two photons in the capture of negative pions by nuclei.[1] Further experiments are in progress or are being planned.[2] The nuclear $(\pi^-, 2\gamma)$ process is interesting for several reasons. As first discussed by Ericson and Wilkin,[3] this reaction can serve as a means to probe the pion content of the nucleus, and it can provide a means to study π-nucleon interactions and pion propagation in the nuclear medium. Barshay[4] has shown further that, with appropriate kinematics, this π-capture process can provide a definite signal for the presence of a pion condensate in a nucleus.

In order to use effectively the $(\pi^-, 2\gamma)$ reaction to study these various nuclear effects it is essential to have an accurate model description of the single-nucleon reaction $\pi^- p \to \gamma\gamma n$. Given the success of a chiral-invariant Lagrangian model for pion photoproduction,[5] it is natural to generalize this approach to the 2γ process. We do this in the present work and derive an expression for the two-photon amplitude which is very similar to that obtained by Lapidus and Musakhanov,[6] who followed the method of Low[7] and Adler and Dothan[8] to derive a low-energy theorem for this reaction. The two-photon amplitude has also been studied recently by Beder,[9] who has considered the effects of the Δ resonance in intermediate states.

Aside from its importance in the analysis of the nuclear $(\pi, 2\gamma)$ reaction, the single-nucleon process is of considerable interest in its own right. One of the diagrams which contributes to the process in the lowest order of α is the virtual charge exchange $\pi^- \to "\pi^0" \to \gamma\gamma$, shown as diagram 10 in Fig. 1. The evaluation of this diagram requires the isoantisymmetric part of the πN amplitude with one pion off the mass shell and a knowledge of the sign of the $\pi^0 \to \gamma\gamma$ amplitude. Both of these factors are of keen theoretical interest. In the literature there are now several theories of the off-mass-shell πN amplitude.[10-12] They tend to differ in dynamical assumptions and, consequently, lead to different predictions for the variation of the amplitude as a pion goes off-shell. An experimental study of a process sensitive to the off-shell amplitude

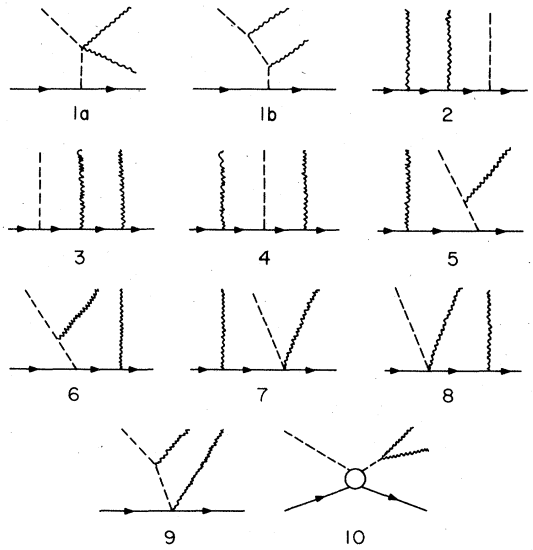

FIG. 1. The tree diagrams for $\pi^- p \to \gamma\gamma n$ which follow from the chiral Lagrangian of Eq. (1). The open circle in diagram 10 represents the pion-nucleon scattering amplitude; the tree diagrams for this amplitude are shown in Fig. 2.

could differentiate between these various models; the $(\pi^-, 2\gamma)$ process seems to be a possible candidate for such a study. The sign of the $\pi^0 \to \gamma\gamma$ amplitude is of interest owing to the work of Adler,[13] who has shown that the sign depends on the charges and axial couplings of the elementary fermions (quarks). Knowledge of the sign and magnitude of the $\pi^0 \to \gamma\gamma$ amplitude provides a way of choosing between different models of the elementary particles, as noted by Okubo.[14] The relative sign between the π^0 decay amplitude and the πN coupling constant has previously been determined by Okubo[14] from analyses of the Compton scattering of a proton and the radiative pion decay $\pi^+ \to e^+\nu\gamma$, and by Gilman[15] from the experimentally observed constructive interference between the amplitude for the Primakoff effect and the other amplitudes involved in π^0 photoproduction. Furthermore, Lapidus and Musakhanov[6] have shown that it is also possible to determine the sign of the two-photon decay amplitude by measuring the neutron energy spectrum in $\pi^- p \to \gamma\gamma n$.

The recent $(\pi^-, 2\gamma)$ experiments[1] detect only the final state γ's which result from the capture of stopped pions on ^{12}C. The reaction occurs with both $1s$- and $2p$-state pions; because of the latter, momentum dependent terms in the amplitude must be included when computing the branching ratio for this process, as discussed by Roberson *et al.*[1] The complete amplitude for $\pi^- p \to \gamma\gamma n$ presented below in Sec. III can be used in the impulse approximation to compute the branching ratio and thereby improve upon the estimates of Ericson and Wilkin.[3] In the present work, however, we study only the single-nucleon reaction with the pion captured in flight. As in the nuclear experiments we assume that only the γ's are observed, and we examine the questions of whether such an experiment can be used to differentiate between various models of the off-mass-shell pion-nucleon amplitude or determine the sign of the amplitude for $\pi^0 \to \gamma\gamma$ decay.

II. CHIRAL LAGRANGIAN

To construct a chiral Lagrangian for $\pi^- p \to \gamma\gamma n$ we make use of the usual chiral Lagrangian for pion-nucleon scattering[16] and introduce a coupling to the electromagnetic field by the minimal substitution. This procedure guarantees that the four-vector potential, A_μ, is coupled to a conserved current, and it therefore preserves gauge invariance. We add terms to the Lagrangian that describe phenomenologically the interaction of the electromagnetic field with the nucleon magnetic moments and the $\pi^0 \to \gamma\gamma$ decay. Our interaction Lagrangian is then

$$
\begin{aligned}
L &= L_{\pi NN} + L_{\gamma\pi NN} + L_{\gamma NN} + L_{\gamma\pi\pi} + L_{\gamma\gamma\pi\pi} + L_{\pi\gamma\gamma}\,,\\
L_{\pi NN} &= \frac{g_\pi}{2M}(\bar N\gamma_5\gamma_\mu\vec\tau N)\cdot\partial^\mu\vec\pi \\
&\quad + \left(\frac{f_0}{m_\pi}\right)^2 \bar N\gamma_\mu\vec\tau N\cdot(\partial^\mu\vec\pi\times\vec\pi)\,,\\
L_{\gamma\pi NN} &= ie\,\frac{g_\pi}{2M}\sqrt{2}\,\bar N\gamma_5 A(\tau_-\pi^- + \tau_+\pi^+)N\,,\\
L_{\gamma NN} &= -eA^\mu\bar N[\tfrac{1}{2}(1+\tau_3)]\gamma_\mu N \\
&\quad -eF^{\mu\nu}\left\{\frac{\kappa_p}{4M}\bar N\sigma_{\mu\nu}[\tfrac{1}{2}(1+\tau_3)]N\right.\\
&\quad \left. + \frac{\kappa_n}{4M}\bar N\sigma_{\mu\nu}[\tfrac{1}{2}(1-\tau_3)]N\right\}, \qquad (1)\\
L_{\gamma\pi\pi} &= ieA^\mu[\pi^+(\partial_\mu\pi^-) - (\partial_\mu\pi^+)\pi^-]\,,\\
L_{\gamma\gamma\pi\pi} &= -e^2A_\mu A^\mu\pi^+\pi^-\,,\\
L_{\pi\gamma\gamma} &= \tfrac{1}{2}e^2F\epsilon_{\alpha\beta\mu\nu}(\partial^\mu A^\alpha)(\partial^\nu A^\beta)\pi_3\,.
\end{aligned}
$$

Our conventions are that $e<0$ and the field $\pi^- = (1/\sqrt{2})(\pi_1 + i\pi_2)$ annihilates (creates) the π^- (π^+) particle state. Our other conventions are generally the same as those of Bjorken and Drell.[17]

To determine the value of the coupling constant f_0 we follow Peccei[5] and Schwinger[18] and require that the chiral current constructed from $L_{\pi NN}$,

$$
\vec J_\mu = \partial_\mu\vec\pi\times\vec\pi + \bar N\gamma_\mu(\tfrac{1}{2}\vec\tau)\left(1 - \frac{g_\pi m_\pi}{2Mf_0}\gamma_5\right)N + \cdots, \qquad (2)
$$

describe the β decay of the nucleon. It follows that

$$
\frac{g_\pi m_\pi}{2Mf_0} = \frac{g_A}{g_V} = 1.25\,. \qquad (3)
$$

With[11] $g_\pi = 12.8$, we have $f_0 = 0.761$.

The π^0 decay constant F is determined, except for sign, from the experimental width Γ_{π^0} for $\pi^0 \to 2\gamma$,

$$
\begin{aligned}
F &= \pm\left(\frac{4\Gamma_{\pi^0}}{\pi\alpha^2 m_{\pi^0}^3}\right)^{1/2} \qquad (4)\\
&= \pm 3.88\times10^{-2} m_\pi^{-1}\,,
\end{aligned}
$$

with[19] $\Gamma_{\pi^0} = 7.95$ eV. (Hermiticity of the Lagrangian requires that F be real.) For completeness we record here the numerical values of other coupling constants and parameters used[19]:

$$
\begin{aligned}
&m_\pi = 139.57\ \text{MeV},\quad m_{\pi^0} = 0.966\,97\ m_\pi\,,\\
&M = 6.7273\ m_\pi\,,\\
&\alpha = e^2/4\pi = 1/137.036\,,\\
&\kappa_p = 1.7928,\quad \kappa_n = -1.9130\,.
\end{aligned} \qquad (5)
$$

Additional terms can be added to the Lagrangian to phenomenologically describe the effects of the nucleon resonances. The $\Delta(1232)$ resonance is expected to be the most important at the energies we consider. However, at present, there is simply no consistent Lagrangian field theory of spin-$\frac{3}{2}$ particles[20]; certain anticommutators which appear in the theory of a quantized, spin-$\frac{3}{2}$ field are necessarily incompatible with a positive-definite metric. Even if one ignores this difficulty, questions of double counting arising from the simultaneous inclusion of both the nucleon and the Δ pole terms still must be dealt with. For these reasons we have not included the nucleon resonances in our Lagrangian. Beder[9] has estimated the size of the Δ intermediate state diagrams in $\pi^- p \to \gamma\gamma n$ using a particular model and has found that near threshold the total Δ amplitude is +7% of the amplitude corresponding to diagram 1 of Fig. 1.

III. REACTION AMPLITUDE

In Fig. 1 we show the tree diagrams for $\pi^- p \to \gamma\gamma n$.[21] The reaction amplitudes for these diagrams are obtained from our Lagrangian by the usual procedure. Writing the S-matrix element with invariantly normalized states as

$$S = (2\pi)^4 \delta^4(p + q - p' - k' - k)\left[\sqrt{2}\ \frac{g_\pi}{2M}(4\pi\alpha)\epsilon'_\nu \epsilon_\mu \sum_{i=1}^{9} M_i^{\nu\mu} + M_{10}\right], \tag{6}$$

we have

$$M_1^{\nu\mu} = \bar{u}'\gamma_5 u\ \frac{2M}{(p'-p)^2 - m_\pi^2}\left[-g^{\mu\nu} + \frac{(2q-k)^\mu(2q-2k-k')^\nu}{(q-k)^2 - m_\pi^2}\right] + (\mu, k \leftrightarrow \nu, k'), \tag{7a}$$

$$M_2^{\nu\mu} = \bar{u}'\not{q}\gamma_5\ \frac{\not{p}' - \not{q} + M}{(p'-q)^2 - M^2}\left(\gamma^\mu - i\ \frac{\kappa_p}{2M}\sigma^{\mu\rho}k_\rho\right)\frac{\not{p} - \not{k}' + M}{(p-k')^2 - M^2}\left(\gamma^\nu - i\ \frac{\kappa_p}{2M}\sigma^{\nu\lambda}k'_\lambda\right)u + (\mu, k \leftrightarrow \nu, k'), \tag{7b}$$

$$M_3^{\nu\mu} = \bar{u}'\left(-\ \frac{i\kappa_n}{2M}\sigma^{\mu\rho}k_\rho\right)\frac{\not{p}' + \not{k} + M}{(p'+k)^2 - M^2}\left(-i\ \frac{\kappa_n}{2M}\sigma^{\nu\lambda}k'_\lambda\right)\frac{\not{p} + \not{q} + M}{(p+q)^2 - M^2}\not{q}\gamma_5 u + (\mu, k \leftrightarrow \nu, k'), \tag{7c}$$

$$M_4^{\nu\mu} = \bar{u}'\left(-\ \frac{i\kappa_n}{2M}\sigma^{\mu\rho}k_\rho\right)\frac{\not{p}' + \not{k} + M}{(p'+k)^2 - M^2}\not{q}\gamma_5\ \frac{\not{p} - \not{k}' + M}{(p-k')^2 - M^2}\left(\gamma^\nu - i\ \frac{\kappa_p}{2M}\sigma^{\nu\lambda}k'_\lambda\right)u + (\mu, k \leftrightarrow \nu, k'), \tag{7d}$$

$$M_5^{\nu\mu} = \bar{u}'\gamma_5(\not{q} - \not{k}')\ \frac{\not{p} - \not{k} + M}{(p-k)^2 - M^2}\left(\gamma^\mu - \ \frac{i\kappa_p}{2M}\sigma^{\mu\lambda}k_\lambda\right)u\ \frac{(2q-k')^\nu}{(q-k')^2 - m_\pi^2} + (\mu, k \leftrightarrow \nu, k'), \tag{7e}$$

$$M_6^{\nu\mu} = \bar{u}'\left(-\ \frac{i\kappa_n}{2M}\sigma^{\mu\rho}k_\rho\right)\frac{\not{p}' + \not{k} + M}{(p'+k)^2 - M^2}\gamma_5(\not{q} - \not{k}')u\ \frac{(2q-k')}{(q-k')^2 - m_\pi^2} + (\mu, k \leftrightarrow \nu, k'), \tag{7f}$$

$$M_7^{\nu\mu} = \bar{u}'\gamma^\mu\gamma_5\ \frac{\not{p} - \not{k}' + M}{(p-k')^2 - M^2}\left(\gamma^\nu - \ \frac{i\kappa_p}{2M}\sigma^{\nu\rho}k'_\rho\right)u + (\mu, k \leftrightarrow \nu, k'), \tag{7g}$$

$$M_8^{\nu\mu} = \bar{u}'\left(-\ \frac{i\kappa_n}{2M}\sigma^{\mu\rho}k_\rho\right)\frac{\not{p}' + \not{k} + M}{(p'+k)^2 - M^2}\gamma^\nu\gamma_5 u + (\mu, k \leftrightarrow \nu, k'), \tag{7h}$$

$$M_9^{\nu\mu} = \bar{u}'\gamma_5\gamma^\mu u\ \frac{(2q-k')^\nu}{(q-k')^2 - m_\pi^2} + (\mu, k \leftrightarrow \nu, k'), \tag{7i}$$

$$M_{10} = \left(-i\sqrt{2}\ T_0^{(-)}\ \frac{e^2 F \epsilon_{\alpha\beta\mu\nu}\epsilon^\alpha \epsilon'^\beta k^\mu k'^\nu}{q'^2 - m_{\pi^0}^2 + i m_{\pi^0}\Gamma_{\pi^0}}\right). \tag{7j}$$

Several remarks are required concerning the last expression. We have modified the π^0 propagator to reflect the finite width by the replacement $m_{\pi^0} \to m_{\pi^0} - \frac{1}{2} i\Gamma_{\pi^0}$. $T_0^{(-)}$ denotes the isoantisymmetric, off-mass-shell πN scattering amplitude. We write this in the form

$$T_0^{(-)} = \bar{u}(p')[A^{(-)}(s,t,u) + \not{q} B^{(-)}(s,t,u)]u(p), \tag{8}$$

with $s=(p+q)^2$, $t=(p'-p)^2$, and $u=(p'-q)^2$. The contributions to the isospin-odd invariant amplitudes $A^{(-)}$ and $B^{(-)}$ coming from our effective Lagrangian can best be separated into two parts. The nucleon exchange diagrams of Figs. 2(a) and 2(b) give

$$A_N^{(-)} = 0, \tag{9a}$$

$$B_N^{(-)} = -2\left(\frac{g_\pi}{2M}\right)^2 - 4M^2\left(\frac{g_\pi}{2M}\right)^2\left(\frac{1}{s-M^2} + \frac{1}{u-M^2}\right), \tag{9b}$$

while the contact diagram [Fig. 2(c)] yields

$$A_C^{(-)} = 0, \tag{10a}$$

$$B_C^{(-)} = 2\left(\frac{f_0}{m_\pi}\right)^2. \tag{10b}$$

The s-wave scattering length $a_S^{(-)} = \frac{1}{3}(a_1 - a_3)$ implied by these amplitudes is

$$\begin{aligned} a_S^{(-)} &= \frac{(A^{(-)} + m_\pi B^{(-)})_{q^2=0}}{4\pi(1+m_\pi/M)} \\ &= \frac{1}{4\pi(1+m_\pi/M)}\left(\frac{2m_\pi^3 g_\pi^2}{4M^2(4M^2-m_\pi^2)} + 2\frac{f_0^2}{m_\pi}\right) \\ &= 0.081 m_\pi^{-1}. \end{aligned} \tag{11}$$

This number is in good agreement with the scattering lengths obtained by fits to the data.[22-24] The predictions of our Lagrangian for the p-wave scattering volumes, however, are poor. The scattering volumes are given by[25]

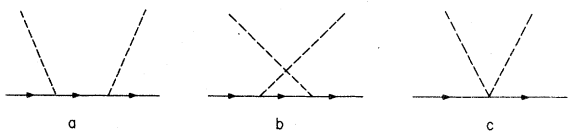

FIG. 2. The tree diagrams for the pion-nucleon scattering amplitude.

$$\begin{aligned} a_{P3/2}^{(-)} &= \tfrac{1}{3}(a_{13} - a_{33}) \\ &= -\frac{g_\pi^2}{24\pi m_\pi M^2(1+m_\pi/M)(1-m_\pi/2M)^2} \\ &= -0.047 m_\pi^{-3}, \end{aligned} \tag{12}$$

$$\begin{aligned} a_{P1/2}^{(-)} &= \tfrac{1}{3}(a_{11} - a_{31}) \\ &= a_{P3/2}^{(-)} - \frac{a_S^{(-)}}{4M^2} + \frac{1}{16\pi M m_\pi} \\ &\quad \times\left(\frac{g_\pi^2 m_\pi^3}{M^2(4M^2-m_\pi^2)} + 4\frac{f_0^2}{m_\pi}\right) \\ &= -0.041 m_\pi^{-3}. \end{aligned} \tag{13}$$

Previous calculations[25,26] of the scattering volumes have included, in various ways, contributions of the $\Delta(1232)$. With such additions reasonable agreement with other determinations of the scattering volumes has been achieved. For example, by including Δ pole diagrams evaluated according to the Lagrangian model of Peccei,[25] we find

$$a_S^{(-)} = 0.082 m_\pi^{-1}, \tag{14a}$$

$$a_{P3/2}^{(-)} = -0.075 m_\pi^{-3}, \tag{14b}$$

$$a_{P1/2}^{(-)} = -0.022 m_\pi^{-3}. \tag{14c}$$

These numbers are in good agreement with the results of Langbein[23] and the compilation of results presented in Nagels *et al.*[24]

Because of the importance of the p waves to the charge-exchange amplitude (even near threshold) and the quality of agreement with the accepted values of the scattering volumes when Δ pole terms are included according to the model of Peccei, we include the Δ contributions to the invariant amplitudes in our $(\pi, 2\gamma)$ calculations. Following Peccei, the contributions of the Δ pole terms to the invariant amplitudes are

$$A_\Delta^{(-)} = \frac{h^2}{3m_\pi^2}\left(\frac{\alpha(s,t)}{s-(M_\Delta - i\frac{1}{2}\Gamma_\Delta)^2} - \frac{\alpha(u,t)}{u-(M_\Delta - i\frac{1}{2}\Gamma_\Delta)^2}\right), \tag{15a}$$

$$B_\Delta^{(-)} = \frac{h^2}{3m_\pi^2}\left(\frac{\beta(s,t)}{s-(M_\Delta - i\frac{1}{2}\Gamma_\Delta)^2} + \frac{\beta(u,t)}{u-(M_\Delta - i\frac{1}{2}\Gamma_\Delta)^2}\right), \tag{15b}$$

where

$$\alpha(s,t) = 8(M_\Delta + M)(t - 2m_\pi^2) + (4M_\Delta + 6M)(s - M^2) + \frac{4}{3M_\Delta}[s^2 - s(M^2 - 4m_\pi^2) - 4m_\pi^2(M^2 - m_\pi^2)] + \frac{2M}{3M_\Delta^2}[3s^2 - s(7M^2 - 8m_\pi^2) + 4(M^2 - m_\pi^2)^2], \tag{16a}$$

$$\beta(s,t) = 2(s - M^2) + 8(t - m_\pi^2) - M(8M_\Delta + 12M) + \frac{8M}{3M_\Delta}(s - 2M^2 + 2m_\pi^2) + \frac{2}{3M_\Delta^2}[s^2 - s(3M^2 - 4m_\pi^2) + 4(M^2 - m_\pi^2)^2]. \tag{16b}$$

The $\pi N\Delta$ coupling constant h is determined from the Δ width by

$$\Gamma_\Delta = \frac{4}{3\pi} h^2 \frac{p^3(E+M)}{M_\Delta m_\pi^2},$$

with E (p) the energy (momentum) of the nucleon in the Δ rest frame. Using[19] $\Gamma_\Delta = 115$ MeV and $M_\Delta = 1232$ MeV gives $h^2 = 0.293$. In our chiral Lagrangian model we have for the invariant amplitudes

$$A^{(-)} = A_\Delta^{(-)}, \tag{17a}$$

$$B^{(-)} = B_N^{(-)} + B_C^{(-)} + B_\Delta^{(-)}. \tag{17b}$$

To illustrate the sensitivity of the $\pi^- p \to \gamma\gamma n$ reaction to the virtual charge-exchange diagram in general and to the model for the off-shell πN amplitude in particular, we have carried out calculations using a different evaluation of the invariant amplitudes. For the physical πN amplitude, A and B have the familiar partial-wave expansions[27]

$$A^{(-)} = 4\pi\left(\frac{W+M}{E+M} f_1^{(-)}(q) - \frac{W-M}{E-M} f_2^{(-)}(q)\right), \tag{18a}$$

$$B^{(-)} = 4\pi\left(\frac{1}{E+M} f_1^{(-)}(q) + \frac{1}{E-M} f_2^{(-)}(q)\right), \tag{18b}$$

where $E = (M^2 + q^2)^{1/2}$ is the energy of the nucleon in the c.m. system and

$$f_1 = \sum_{l=0}^{\infty} f_{l+} P'_{l+1}(x) - \sum_{l=2}^{\infty} f_{l-} P'_{l-1}(x), \tag{19a}$$

$$f_2 = \sum_{l=1}^{\infty} (f_{l-} - f_{l+}) P'_l(x). \tag{19b}$$

x is the cosine of the c.m. scattering angle, $P'_l(x)$ is the first derivative of the conventionally normalized Legendre polynomial, and $f_{l\pm}$ is the partial-wave amplitude in the state of parity $-(-1)^l$ and total angular momentum $j = l \pm \frac{1}{2}$ which is related to phase shifts by

$$f_{l\pm} = \frac{1}{q} e^{i\delta_{l\pm}} \sin\delta_{l\pm}. \tag{20}$$

For the πN amplitude with one pion off the mass shell these expressions must be suitably modified. We let $\vec{l}_1$ ($\vec{l}_2$) denote the c.m. momentum for the πN state with the on-shell (off-shell) pion, and define the nucleon energies $E_i = (M^2 + l_i^2)^{1/2}$. In terms of the Lorentz scalars s, t, and u, defined earlier,

$$|\vec{l}_1| = \left[\tfrac{1}{4}s - \tfrac{1}{2}(M^2 + m_\pi^2) + \frac{1}{4s}(M^2 - m_\pi^2)^2\right]^{1/2}, \tag{21a}$$

$$|\vec{l}_2| = \left[\frac{1}{4s}(3M^2 + m_\pi^2 - t - u)^2 - M^2\right]^{1/2}, \tag{21b}$$

$$\vec{l}_2 \cdot \vec{l}_1 = \tfrac{1}{2}t - M^2 + E_1 E_2. \tag{21c}$$

The A and B amplitudes with an off-shell pion become[28]

$$A^{(-)} = \frac{4\pi(W+M)}{[(E_1+M)(E_2+M)]^{1/2}} \times\left(f_1^{(-)}(l_2, l_1) - \frac{W-M}{W+M}\frac{(E_1+M)(E_2+M)}{l_2 l_1} f_2^{(-)}(l_2, l_1)\right), \tag{22a}$$

$$B^{(-)} = \frac{4\pi}{[(E_1+M)(E_2+M)]^{1/2}} \times\left(f_1^{(-)}(l_2, l_1) + \frac{(E_1+M)(E_2+M)}{l_2 l_1} f_2^{(-)}(l_2, l_1)\right). \tag{22b}$$

f_1 and f_2 are now expressed in terms of the two variable partial-wave amplitudes $f_{l\pm}(l_2, l_1)$, where

$$f_{l\pm}(l_1, l_1) = \frac{1}{l_1} e^{i\delta_{l\pm}} \sin\delta_{l\pm} \tag{23}$$

in the normal fashion. For the s waves we use the off-shell partial-wave amplitudes constructed by Banerjee and Cammarata[11] from the nonlinear Low equation. On-shell these amplitudes agree well over the elastic scattering region with the phase shifts of Carter, Bugg, and Carter.[29] The amplitudes imply an isospin-odd s-wave scattering length

$$a_S^{(-)} = 0.079 m_\pi^{-1}. \tag{24}$$

For the half-off-mass-shell p-wave amplitudes we use the factorable form[11]

$$f_\nu(l_2, l_1) = \frac{l_2\phi(l_2)}{l_1\phi(l_1)} f_\nu(l_1, l_1), \tag{25}$$

$$\nu = (P_{11}, P_{13}, P_{31}, P_{33}).$$

The form factor $\phi(l)$ is parametrized as

$$\phi(l) = \left(1 + \frac{l^2}{\mu^2}\right)^{-5/2}, \tag{26}$$

with $\mu = 8m_\pi$, as in Ref. 11. The on-shell p-wave amplitudes are constructed using the fits to the p-wave phase shifts developed by Salomon.[22] These imply

$$a^{(-)}_{P3/2} = -0.074 m_\pi^{-3}, \tag{27a}$$

$$a^{(-)}_{P1/2} = -0.006 m_\pi^{-3}. \tag{27b}$$

IV. NUMERICAL RESULTS

All of our calculations of $\pi^- p \to \gamma\gamma n$ have been for the lab frame, in which the target proton is at rest. We assume that the momentum vector of the incident pion is directed toward the positive z axis and that the proton is at the origin of coordinates. The various angular variables for the photons are defined in Fig. 3.

As mentioned in the Introduction, our numerical study is for an experiment in which only the final state photons are detected, and we have explored the feasibility of using such an experiment to determine the sign of the amplitude for the two-photon decay of the π^0 and the behavior of the πN charge-exchange amplitude as one pion goes off the mass shell. In regard to the latter, several results follow immediately from a study of the virtual charge-exchange amplitude of Eq. (7j). First we note that the squared four-momentum of the π^0 can be expressed in terms of the photon variables as

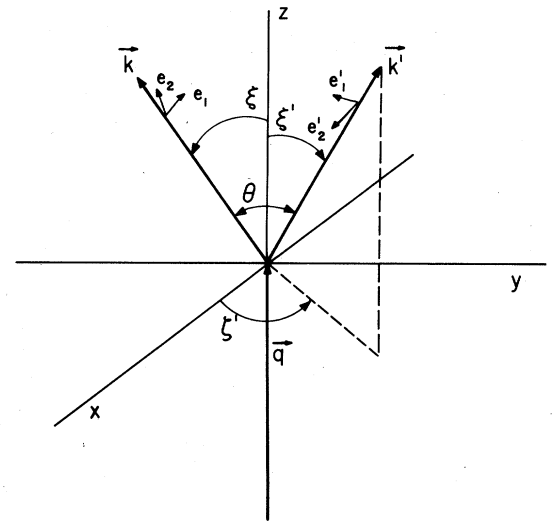

FIG. 3. The coordinate system used in the calculations. $\vec{q}$ is the three-momentum of the incident π^- in the lab. The photon three-momentum $\vec{k}$ lies always in the x-z plane, as does the polarization unit vector $\hat{e}_1$. $\hat{e}_1$, $\hat{e}_2$, and $\hat{k}$ form an orthonormal set, with $\hat{e}_2 = \hat{k}x\hat{e}_1$. The polarization vector $\hat{e}'_1$ lies always in the $\hat{k}'-z$ plane. $\hat{e}'_1$, $\hat{e}'_2$, and $\hat{k}'$ also form an orthonormal set with $\hat{e}'_2 = \hat{k}' \times \hat{e}'_1$.

$$q'^2 = 2\omega\omega'(1 - \cos\theta). \tag{28}$$

Energy-momentum conservation implies that, in the lab frame, the energies of the photons are related by

$$\omega' = \frac{W^2 - M^2 - q^2 + 2\omega(q\cos\xi - W)}{2[W - q\cos\xi' - \omega(1 - \cos\theta)]}, \tag{29}$$

where q is the three-momentum of the π^- and $W = M + (m_\pi^2 + q^2)^{1/2}$. These equations show that for fixed W, ξ, and ξ', the π^0 is farthest from the mass shell for $\theta = 0$ or 180°. However, the structure of the $\pi^0 \to \gamma\gamma$ vertex factor is such that it tends to suppress the virtual charge-exchange amplitude as the π^0 goes off-shell with small θ. By expanding the factor $\epsilon_{\alpha\beta\mu\nu}\epsilon^\alpha \epsilon'^\beta k^\mu k'^\nu$ into components one sees that the π^0 decay vertex involves the unit vectors for photon momentum and polarization in the form

$$\hat{e} \times \hat{e}' \cdot (\hat{k} - \hat{k}'). \tag{30}$$

This shows that for a given polarization for each photon, the magnitude of the vertex decreases as θ decreases. Furthermore, if the polarizations of the photons are not measured, there is an additional suppression of diagram 10, for small θ, coming from the polarization sum

$$\sum_{\text{pol}} |M_{10}|^2 \sim (1 - \cos\theta)^2. \tag{31}$$

Our numerical work is, of course, consistent with these observations. We find that for kinematic configurations in which the charge-exchange process with virtual π^0's plays a non-negligible role the cross sections are on the order of 1 pb per MeV near threshold. Examples are shown in Fig. 4, where we display differential cross sections in which the angles, energies, and polarizations of the photons are measured. Curve a includes diagrams 1–9 of Fig. 1, curve b includes all 10 diagrams with the invariant amplitudes of Eq. (22), while curve c shows the effect of using the chiral Lagrangian model for the invariant amplitudes. The two models generally give significantly different invariant amplitudes above threshold. The average values of the invariant amplitudes of Eq.

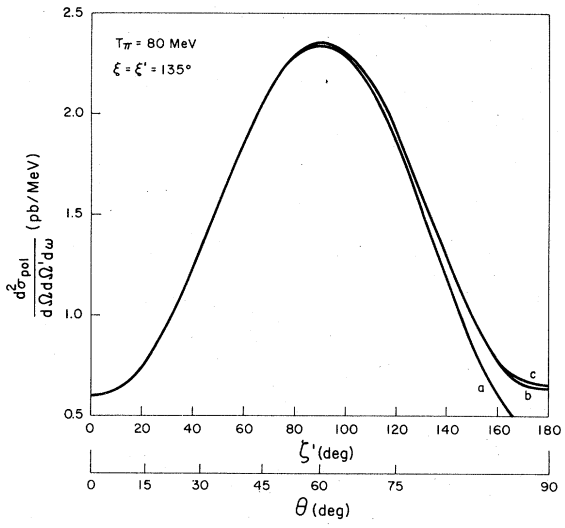

FIG. 4. Differential cross sections in the lab frame with definite polarization states for the photons. T_π is the π^- kinetic energy in the lab. Curve *a* corresponds to diagrams 1–9, curve *b* to diagrams 1–10 with the invariant amplitudes of Eq. (22), and curve *c* to diagrams 1–10 with the chiral Lagrangian results for the invariant amplitudes, with the Δ terms included. The energy of one photon is fixed at $\omega = 71.3$ MeV, while the energy of the second photon spans the range $\omega' = 107.0$–113.3 MeV as θ goes from 0 to 90°. The polarization states of the γ's correspond to e_1 and e_2' of Fig. 3.

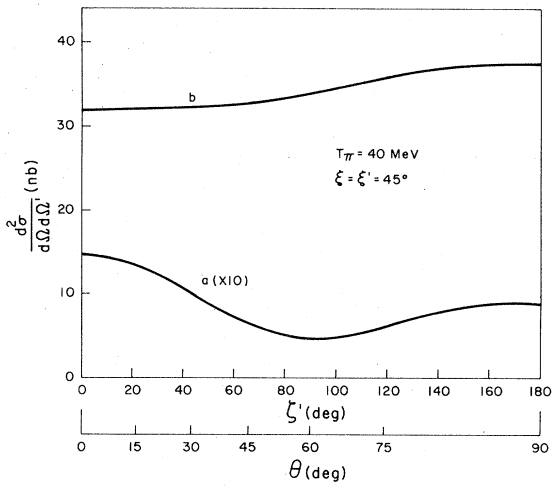

FIG. 5. Differential cross sections in the lab frame summed over photon polarizations and energies with $\omega_{min} = 10$ MeV. Curve *a* includes only diagram 1 and is shown scaled by the factor 10. Curve *b* includes diagrams 1–10 with the invariant amplitudes of Eq. (22). The contribution of diagram 10 to curve *b* is negligibly small.

(17) over the range $\theta = 0 - 90°$ for the kinematics of Fig. 4 are

$$A_{av}^{(-)} = (-11.2 - 5.6i)m_\pi^{-1}, \tag{32a}$$

$$B_{av}^{(-)} = (10.9 + 4.9i)m_\pi^{-2}, \tag{32b}$$

while for the amplitudes of Eq. (22) we find

$$A_{av}^{(-)} = (-16.1 - 3.9i)m_\pi^{-1}, \tag{33a}$$

$$B_{av}^{(-)} = (14.3 + 3.2i)m_\pi^{-2}. \tag{33b}$$

The curves in Fig. 4 illustrate the numerically insignificant effects of diagram 10 with an off-shell pion. Hence we conclude that it is not feasible to differentiate between even very different models of the off-shell amplitude with experiments that detect the final photons.

Figure 5 displays differential cross sections at 40 MeV incident pion kinetic energy (lab) that are summed over photon polarizations and partially summed over photon energies. In performing the integration over photon energies we have assumed that photons with energy less than $\omega_{min} = 10$ MeV are not detected. If one computes cross sections summed over energy using only the diagrams of Fig. 1 some lower limit on the photon energy must be assumed, when $T_\pi > 0$, since several of the diagrams are infrared divergent. We note that if ω_{min} is increased to 20 MeV, the cross section shown as curve *b* in Fig. 5 decreases by about 40%. As illustrated in this figure, the cross section obtained using only diagram 1 is more than an order of magnitude smaller than the one computed with all tree diagrams.

In general, when $\theta > 90°$, the integrations over photon energy include two energies at which the real part of the denominator in M_{10} vanishes. Because of the smallness of the $\pi^0 \to \gamma\gamma$ width the integrated cross sections are dominated by the virtual charge-exchange process with the π^0 propagator effectively just $1/m_{\pi^0}\Gamma_{\pi^0}$. In Fig. 6 we show cross sections summed over photon polarizations and energies ($\omega_{min} = 10$ MeV) for an incident pion kinetic energy of 40 MeV and with the photons detected in the plane perpendicular to the incident beam. To carry out the energy integrations for angles θ such that the real part of the denominator in M_{10} has a zero in the range of integration, we factored out of the integrals the numerator of the integrands, evaluated at the energy where the real part of the denominator vanishes, and then performed the integration over the denominator analytically. The left part of Fig. 6 shows the cross section for diagrams 1–10 for the range of θ over which $q'^2 \neq m_{\pi^0}^2$ for all photon energies. In the right part of the figure we show the cross section computed according to the above mentioned procedure. Over the range of integration, $q'^2 = m_{\pi^0}^2$ for two different

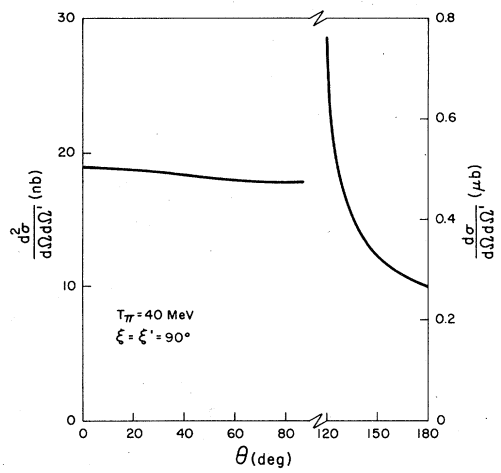

FIG. 6. Differential cross sections in the lab frame summed over photon polarizations and energies with $\omega_{min} = 10$ MeV. The cross section includes diagrams 1–10 with the invariant amplitudes of Eq. (22).

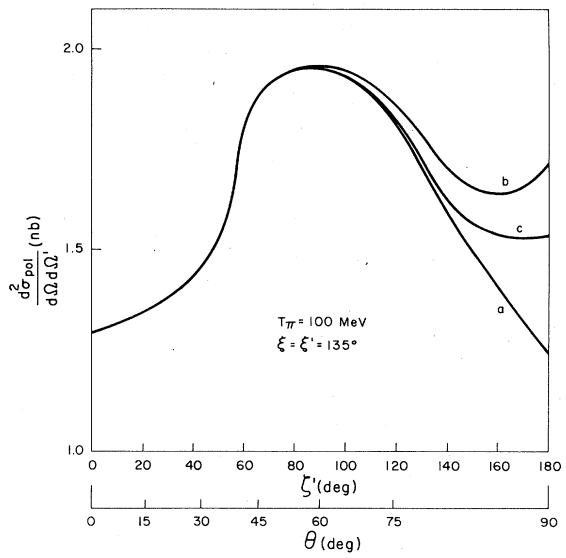

FIG. 7. Differential cross sections in the lab frame summed over photon energies ($\omega_{min} = 10$ MeV) but with definite polarization states for the photons. The polarizations correspond to e_1 and e_2' of Fig. 3. Curve *a* represents diagrams 1–9, and curve *b* includes diagrams 1–10 with the invariant amplitudes of Eq. (22) and with $Fg_\pi < 0$. Curve *c* shows the effect of changing the sign of F.

values of ω for each value of θ in the range 120–180°. The cross section for these values of θ is determined entirely from the charge-exchange diagram; even the interference term between diagrams 1–9 and 10 is negligible, since it is proportional to Γ_{π^0}.

We now consider the feasibility of using $\pi^- p \to \gamma\gamma n$ to determine the sign of the $\pi^0 \to \gamma\gamma$ amplitude. Clearly, we are interested in the interference between diagrams 1–9 with diagram 10. Except near the kinematic points where $q'^2 \simeq m_{\pi^0}^2$, the magnitude of diagram 10 is small compared to that of the sum of the other diagrams, and the interference term is also small. Since the Lagrangian model we have developed becomes inaccurate at the higher energies where effects of the nucleon resonances become important, we have limited our numerical study to incident pions with kinetic energy in the lab of not more than 100 MeV (where $\sqrt{s} = 1160$ MeV). Differential cross sections at this uppermost energy are shown in Fig. 7. Curve *a* represents diagrams 1–9, while *b* includes diagram 10 evaluated with the invariant amplitudes of Eq. (22). In computing this cross section we used the negative sign in the $\pi^0 \to \gamma\gamma$ vertex factor of Eq. (4). This sign is also the one we used in computing the cross sections shown in the other figures. Curve *c* of Fig. 7 shows the effect of reversing the sign of the π^0 decay amplitude: The cross section decreases by, at most, 10%. At threshold, however, the effect is much greater, as shown in Fig. 8. Here we display the double differential cross section for the two-γ process divided by the total cross section for $\pi^- p \to \gamma n$. The latter is given by

$$\sigma_\gamma = \frac{1}{v} \frac{M^2(M+2m_\pi)}{8\pi(M+m_\pi)^2 m_\pi} 2\left(\sqrt{2}\,\frac{g_\pi}{2M} e\right)^2,$$

where v is the velocity of the incident pion. The

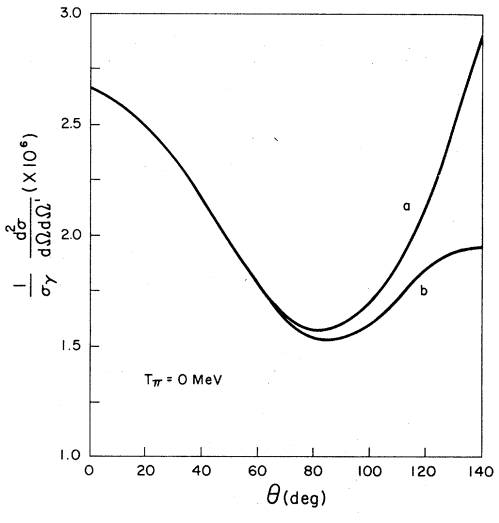

FIG. 8. Differential cross sections in the lab frame at $T_\pi = 0$ MeV normalized to the total cross section for $\pi^- p \to \gamma n$. Curves *a* and *b* include all diagrams; in *a*, $Fg_\pi > 0$, while in *b* $Fg_\pi > 0$. When $\theta > 140°$, $q'^2 = m_{\pi^0}^2$ in the range of integration over the photon energy. The cross section is consequently dominated by diagram 10 and is similar to the one shown in Fig. 6.

magnitude of these cross sections suggests that the sign of the π^0 decay amplitude can be determined from experiments which detect the final photons.

In their paper on $\pi^- p \to \gamma\gamma n$, Lapidus and Musakhanov[6] suggested that the sign of the π^0 amplitude could be determined by a measurement of the neutron spectrum when pions were captured at rest. For completeness, we show in Fig. 9 the cross section, for both signs of F, for detection of the final neutron, again normalized with the one-γ process. The large cross section at the neutron kinetic energy[30] $T_n \simeq 600$ keV results from the vanishing of $q'^2 - m_{\pi^0}{}^2$ in diagram 10. Because of the order of magnitude difference between curves a and b (which differ in the sign of F), it is clear that a measurement of the neutron spectrum can also determine the sign of the π^0 decay amplitude.

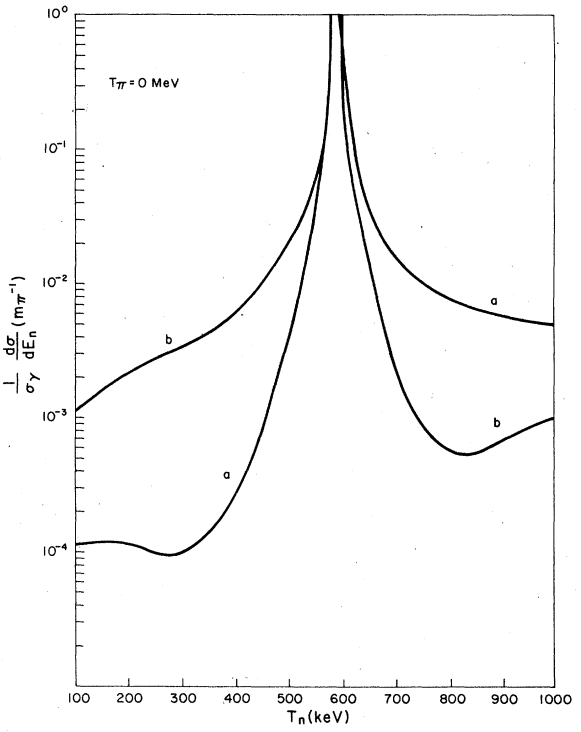

FIG. 9. Differential cross sections in the lab at $T_\pi = 0$ MeV for detecting the final neutron. $E_n = T_n + M$, where T_n is the neutron's kinetic energy. Curves a and b include all diagrams; in a, $Fg_\pi < 0$, while in b, $Fg_\pi > 0$.

V. SUMMARY AND CONCLUSIONS

In analogy with the work of Peccei[5] on pion photoproduction, we have constructed a chiral Lagrangian model for $\pi^- p \to \gamma\gamma n$. Our evaluation of the tree diagrams for this process leads to a reaction amplitude which is similar to the one derived by Lapidus and Musakhanov[6] using a low-energy theorem.

The main diagram of interest in our study describes the charge-exchange process π^- – virtual $\pi^0 \to \gamma\gamma$. This diagram involves directly the sign of the $\pi^0 \to \gamma\gamma$ decay amplitude and the pion-nucleon amplitude with one pion off the mass shell. Our numerical work has been based on an assumed experiment in which only the final-state γ's are detected, and we have explored the feasibility of using such an experiment to (1) differentiate between different models of the off-mass-shell πN amplitude, and (2) determine the sign of the $\pi^0 \to \gamma\gamma$ amplitude.

Our principal conclusions are that (1) only in an experiment in which the polarizations and energies of the γ's are measured can the contribution of the virtual charge-exchange process be large relative to the bremsstrahlung terms when $q_{\pi^0}{}^2 < 0.9 m_\pi{}^2$; (2) this reaction is not a practicable way to distinguish between different models of the off-mass-shell amplitude since cross sections are ~1 pb/MeV for kinematic configurations in which the charge-exchange process with virtual π^0's plays a non-negligible role; and (3) a reasonably accurate experiment could determine the sign of the π^0 decay amplitude.

The author thanks Professor D. A. Jenkins for calling his attention to the experiments on $(\pi^-, 2\gamma)$ and for several conversations. He is also grateful to J. Kim for his help in the early stages of this work, and to Professor R. H. Hackman for helpful conversations. This work was supported in part by the National Science Foundation under Grant No. PHY 77-04408.

[1] J. Deutsch *et al.*, Phys. Lett. 80B, 347 (1979); P. L. Roberson *et al.*, Phys. Lett. 70B, 35 (1977).
[2] M. Salomon, private communication.
[3] T. E. O. Ericson and C. Wilkin, Phys. Lett. 57B, 345 (1975).
[4] S. Barshay, Phys. Lett. 78B, 384 (1978).
[5] R. D. Peccei, Phys. Rev. 181, 1902 (1969).
[6] L. I. Lapidus and M. M. Musakhanov, Yad. Fiz. 15, 1002 (1972) [Sov. J. Nucl. Phys. 15, 558 (1972)].
[7] F. E. Low, Phys. Rev. 110, 974 (1958).
[8] S. L. Adler and Y. Dothan, Phys. Rev. 151, 1267 (1966).
[9] D. Beder, University of British Columbia report, 1978 (unpublished).
[10] M. K. Banerjee and J. B. Cammarata, Phys. Rev. D 16, 1334 (1977).
[11] M. K. Banerjee and J. B. Cammarata, Phys. Rev. C 17,

1125 (1978).
[12]D. J. Ernst, J. T. Londergan, E. J. Moniz, and R. M. Thaler, Phys. Rev. C 10, 1708 (1974); L. C. Liu and C. M. Shakin, *ibid.* 18, 604 (1978); M. J. Reiner, Phys. Rev. Lett. 38, 1467 (1977).
[13]S. L. Adler, Phys. Rev. 177, 2426 (1969).
[14]S. Okubo, Phys. Rev. 179, 1629 (1969).
[15]F. Gilman, Phys. Rev. 184, 1964 (1969).
[16]S. Weinberg, Phys. Rev. Lett. 18, 188 (1967); S. Weinberg, Phys. Rev. 166, 1568 (1968).
[17]J. D. Bjorken and S. D. Drell, *Relativistic Quantum Fields* (McGraw-Hill, New York, 1965).
[18]J. Schwinger, Phys. Rev. 167, 1432 (1968).
[19]Particle Data Group, Phys. Lett. 75B, 1 (1978).
[20]C. R. Hagen, Phys. Rev. D 4, 2204 (1971); L. M. Nath, B. Etemadi, and J. D. Kimel, *ibid.* 3, 2153 (1971); K. Johnson and E. C. G. Sudarshan, Ann. Phys. (N.Y.) 13, 126 (1961).
[21]In conformity with the labeling in Ref. 6 we refer to the first two diagrams in Fig. 1 as diagram 1.
[22]M. Salomon, TRIUMF Report No. TRI-74-2 (unpublished). See also G. Rowe, M. Salomon, and R. H. Landau, Phys. Rev. C 18, 584 (1978).
[23]W. Langbein, Nucl. Phys. B94, 519 (1975).
[24]M. M. Nagels *et al.*, Nucl. Phys. B109, 1 (1976).
[25]R. D. Peccei, Phys. Rev. 176, 1812 (1968).
[26]H. Schnitzer, Phys. Rev. 158, 1471 (1967); K. Raman, *ibid.* 164, 1736 (1967).
[27]G. F. Chew, M. L. Goldberger, F. E. Low, and Y. Nambu, Phys. Rev. 106, 1337 (1957).
[28]These expressions for the A and B amplitudes have also been used in a study of pion absorption by deuterons by R. H. Hackman, Phys. Rev. C 19, 1873 (1979).
[29]J. R. Carter, D. V. Bugg, and A. A. Carter, Nucl. Phys. B58, 378 (1973).
[30]Using $M_p = 6.7227 m_\pi$, $M_n = 6.7319 m_\pi$, the peak occurs at 420 keV.